Available online at www.sciencedirect.com

SciVerse ScienceDirect

journal homepage: www.elsevier.com/locate/he

On the effective Lewis number formulations for lean hydrogen/hydrocarbon/air mixtures

Nicolas Bouvet [a,*], Fabien Halter [b], Christian Chauveau [c], Youngbin Yoon [a]

[a] School of Mechanical and Aerospace Engineering, Seoul National University, Seoul 151-742, Republic of Korea
[b] Université d'Orléans, Laboratoire PRISME, 8 rue Léonard de Vinci, 45072 Orléans cedex 2, France
[c] Centre National de la Recherche Scientifique, Institut de Combustion, Aérothermique, Réactivité et Environnement, 1C, avenue de la Recherche Scientifique, 45071 Orléans cedex 2, France

ARTICLE INFO

Article history:
Received 5 December 2012
Received in revised form
8 February 2013
Accepted 22 February 2013
Available online 2 April 2013

Keywords:
Effective Lewis number
Outwardly propagating flame
Burned Markstein length
Hydrogen/hydrocarbon combustion
Syngas combustion

ABSTRACT

Decades of research have underlined the undeniable importance of the Lewis number (*Le*) in the premixed combustion field. From early experimental observations on laminar flame propagation to the most recent DNS studies of turbulent flames, the unbalanced influence of thermal to mass diffusion (i.e. $Le \neq 1$), known as nonequidiffusion, has shed the light on a wide range of combustion phenomena, especially those involving stretched flames. As a result the determination of the Lewis number has become a routine task for the combustion community. Recently, the growing interest in hydrogen/hydrocarbon (HC) fuel blends has produced extensive studies that have not only improved our understanding of H_2/HC flame dynamics, but also, in its wake, raised a fundamental question: which effective Lewis number formulation should we use to characterize the combustion of hydrogen/hydrocarbon/air blends? While the Lewis number is unambiguously defined for combustible mixtures with a single fuel reactant, the literature is unclear regarding the appropriate equivalent formulation for bi-component fuels. The present paper intends to clarify this aspect. To do so, effective Lewis number formulations for lean ($\varphi = 0.6$ and 0.8) premixed hydrogen/hydrocarbon/air mixtures have been investigated in the framework of an existing outwardly propagating flame theory. Laminar burning velocities and burned Markstein lengths of H_2/CH_4, H_2/C_3H_8, H_2/C_8H_{18} and H_2/CO fuel blends in air were experimentally and numerically determined for a wide range of fuel compositions (0/100% → 100/0% H_2/HC). By confronting the two sets of results, the most appropriate effective Lewis number formulation was identified for conventional H_2/HC/air blends. Observed deviations from the validated formulation are discussed for the syngas (H_2/CO) flame cases.

Copyright © 2013, Hydrogen Energy Publications, LLC. Published by Elsevier Ltd. All rights reserved.

1. Introduction

The Lewis number *Le*, named in honor of Warren K. Lewis for his pioneering studies on liquid evaporation [1], is nowadays commonly defined as the ratio of the Schmidt to the Prandtl number [2]. It is no surprise that *Le* has tremendous importance for the characterization of transport processes arising in gaseous mixtures, especially in the field of premixed combustion. In this domain, *Le* is equivalently taken as the ratio of the thermal diffusivity (D_T) to the mass diffusivity of the

* *Corresponding author*. Tel.: +82 2 880 7396; fax: +82 2 872 8032.
E-mail address: bouvet@snu.ac.kr (N. Bouvet).

0360-3199/$ – see front matter Copyright © 2013, Hydrogen Energy Publications, LLC. Published by Elsevier Ltd. All rights reserved.
http://dx.doi.org/10.1016/j.ijhydene.2013.02.098

Table 1 – Effective Lewis number formulations for bi-component fuels.

	Le_{eff}	H_2/HC [Ref.]
Heat release-based (H)	$Le_H = 1 + \frac{q_1(Le_1 - 1) + q_2(Le_2 - 1)}{q_1 + q_2}$ (1)	H_2/C_3H_8 [20–22] H_2/CH_4 [14,23] H_2/CO [24,26–29] various HCs [25,28]
Volume-based (V)	$Le_V = x_1 Le_1 + x_2 Le_2$ (2)	H_2/C_3H_8 [32] H_2/CH_4 [14,32]
Diffusion-based (D)	$Le_D = \frac{D_T}{x_1 D_{1/N_2} + x_2 D_{2/N_2}}$ (3)	H_2/CH_4 [14,34] H_2/CO [27]

q_i, non-dimensional heat release corresponding to the fuel species "i"; x_i, fuel volumetric fraction of the component "i"; other parameters as defined in Section 3.2.

deficient reactant (D_i).[1] Decades of combustion research have underlined the salient character of *Le*. Early experimental observations on the propagation, stability and extinction characteristics of laminar flames (e.g., [3–6],), supported by the development of asymptotic theories (e.g., [7–9]), have provided evidence that unequal heat and species diffusion (i.e. $Le \neq 1$) could strongly affect the combustion intensity in the presence of flame stretch (flow straining, flame curvature). This has led to a comprehensive understanding of the dynamics of a broad range of laboratory flames, insightfully reviewed in [10]. The relevance of *Le* in premixed combustion goes clearly beyond the laminar flame regime: a marked sensitivity of global turbulent flame characteristics to *Le* has been previously reported in the course of experimental studies [11–14]; state of the art DNS investigations of turbulent nonequidiffusive mixtures evidenced a local burning reduction/enhancement due to flame curvature effects [15,16]. The determination of a reasonably accurate Lewis number is therefore essential in order to predict and interpret a wide range of combustion phenomena.

Recently, considerable effort has been devoted to the determination of the fundamental combustion characteristics of hydrogen/hydrocarbon (HC)/air blends, since hydrogen additions in lean hydrocarbon mixtures were found to extend the lean operating limits and hence, to lower the pollutant formation in internal combustion engines [17,18]. Moreover, small hydrocarbon additions in hydrogen can potentially mitigate the risks inherent to the high reactivity of hydrogen [19]. The revival of interest in syngas mixtures (H_2/CO)[2] has also sustained this effort. While defining a Lewis number for a mixture with a single fuel is quite straightforward (see discussion above), the definition of an equivalent Lewis number for a mixture with two fuel components is not trivial, and consensus on an adequate formulation still has still to be reached. The combustion literature reports several "effective" Lewis number formulations (Le_{eff}), herein summarized in Table 1. The first expression, i.e. Eq. (1), was introduced by Law and coworkers [20] in their investigation of the cellular instability of high pressure H_2/C_3H_8 laminar spherical flames. Eq. (1) is a weighted average of the Lewis numbers of the two fuels based on their respective non-dimensional heat release. This formulation was extensively used in subsequent studies [14,21–29] and extended to three fuel species [30,31] in order to, in fine, comment on the thermodiffusive stable ($Le > 1$) or unstable ($Le < 1$) character of H_2/HC/air flames. Although rigorously derived from asymptotic analysis, attempts to experimentally validate Eq. (1) have not yet been reported. Since the pioneering approach of Ref. [20], two additional Le_{eff} expressions have been tested in the framework of turbulent premixed combustion. In their computational study of H_2/CH_4–H_2/C_3H_8 turbulent flames [32], Muppala et al. used a volumetric fraction-weighted average formulation, as shown in Eq. (2). When fitted in their chosen flame surface wrinkling model (see AFSW model, Ref. [33]), Eq. (2) led to a fair agreement with experimental burning velocities, although a progressive underestimation at higher turbulent intensities ought to be mentioned. Related work by Dinkelacker et al. [14,34] subsequently investigated a third Le_{eff} approach. Assuming that positively curved flame elements dominate turbulent flame propagation, an enrichment of the flame leading edge in the most diffusive fuel was hypothesized. The resulting Le_{eff} should accordingly depend on a volumetric fraction-weighted average of the fuel diffusivities, see Eq. (3). When inserted in RANS simulations through a *Le*-dependant flame wrinkling ratio [33], this formulation, as compared to the others, led to improved predictions of H_2/CH_4 turbulent flame heights [14]. Although not theoretically derived, Eqs. (2) and (3) deserve particular attention for the following reasons: (i) the simplicity of Eq. (2), stemming from intuitive reasoning, is very attractive as a cost-effective implementation of Le_{eff} in combustion codes; (ii) Eq. (3) is heuristically derived on the assumption that flame curvature is dominant. Thus the broad validity of Eq. (3) is not ensured and deserves to be further investigated; (iii) validations performed in Refs. [14,32] involve a large number of adjustable or empirical parameters (e.g., turbulence and flame wrinkling models) and are, therefore, far from being straightforward. Additional insight could be gained by studying the relative performances of Eqs. (2) and (3) for constrained problems, i.e. simpler flame configurations.

Fig. 1 shows that Eqs. (1)–(3) yield markedly different Le_{eff} values. For instance, a 50/50% H_2/C_3H_8 blend at equivalence ratio 0.6 would be characterized by a Le_H, Le_V and Le_D of 1.77, 1.20 and 0.51, respectively. The span of Le_{eff} above and below

[1] The deficient reactants being the fuel and oxidizer species for lean and rich mixtures, respectively.

[2] CO will be here improperly included in the term "hydrocarbon" for ease of designation.

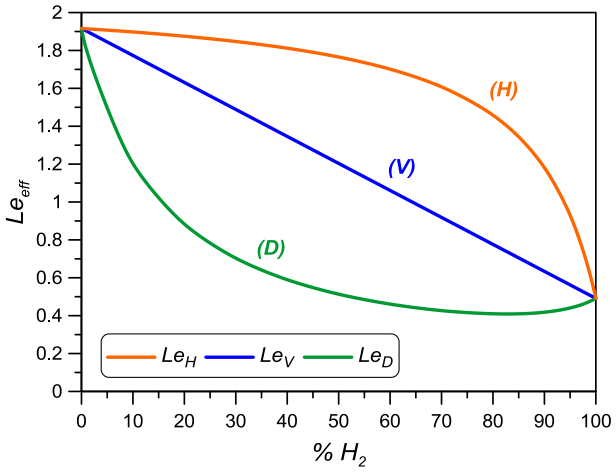

Fig. 1 – Effective Lewis number formulations for H_2/C_3H_8/air flames versus H_2 fuel volumetric content ($\varphi = 0.6$, $T_u = 298$ K).

unity suggests that opposite conclusions could be reached regarding the flame dynamics [10] (i.e. sensitivity to stretch and stability). This observation generally holds for hydrogen/hydrocarbon blends, from lighter (e.g., CH_4) to heavier (e.g., C_8H_{18}) alkanes. Acknowledging the apparent incompatibility of the different models presented in Table 1, we propose here to further investigate their validity in the framework of the Outwardly Propagating Flame (OPF) theory. This approach has led to intense research in the past few years and a non-linear equation governing the laminar spherical flame propagation has subsequently emerged [35–37]:

$$\left(\frac{s_b}{s_b^0}\right)^2 \ln\left(\frac{s_b}{s_b^0}\right)^2 = -2\frac{L_b\kappa}{s_b^0} \quad (4)$$

with s_b and s_b^0, the stretched and unstretched propagation flame speeds respectively, κ, the stretch rate; L_b, the burned Markstein length, which quantifies the flame sensitivity to stretch. Following the analytical developments of Chen et al. [37–39], L_b can be explicitly retrieved as a function of fundamental flame parameters:

$$L_b = \left[\frac{1}{Le} - \left(\frac{Ze}{2}\right)\left(\frac{1}{Le} - 1\right)\right]\sigma\delta \quad (5)$$

with Ze, the flame Zel'dovich number, σ, the flame expansion ratio and δ, the flame thickness. Eq. (5) shows that L_b strongly depends on Le, as predicted by early flame asymptotic theories [8,40]. Bearing in mind that successful extractions of Lewis numbers have been previously performed for single fuel mixtures in the framework of both flame integral analysis [41,42] and asymptotic theory [43], the following methodological approach is proposed in order to identify the appropriate Le_{eff} for lean H_2/HC/air blends:

1. Burned Markstein lengths of various H_2/HC/air blends were experimentally determined based on Eq. (4). A wide range of hydrocarbons, including methane (literature data only), propane, iso-octane and carbon monoxide was considered. The volumetric hydrogen content in the fuel was varied from 0 to 100% at a constant, lean equivalence ratio ($\varphi = 0.6$ or 0.8).
2. The corresponding Markstein lengths were subsequently calculated using Eq. (5). The flame parameters Ze, σ and δ are well defined and can be determined using conventional flame modeling programs incorporating detailed chemistry. The Lewis number Le for a single fuel reactant was alternatively replaced by the Le_{eff} expressions given in Table 1.
3. The relevance of the different Le_{eff} formulations was analyzed by comparing both experimental and calculated Markstein lengths, including previously reported datasets.

2. Experimental methodology

The laminar flame speed measurements were performed in a 4.2 L stainless steel spherical chamber equipped with four optical accesses. Flames were centrally ignited by two tungsten electrodes (1 mm gap), connected to a conventional capacitive discharge system. Prior to ignition the following procedure was systematically observed: the auto-regulated chamber temperature was set at the desired value and a vacuum was created. The gases, and when necessary, liquid iso-octane were injected using calibrated mass flow controllers (Brooks 5850S) and a Coriolis mass flow meter (Bronkhorst Mini-Coriflow) respectively. An electric fan located inside the chamber ensured the homogenous mixing of the reactants. When the filling sequence had been completed, the fan was stopped and the ignition sequence was triggered only when quiescent flow conditions were achieved. Note here that all experiments used synthetic air (20.5/79.5% O_2/N_2). Data acquisition was performed at constant chamber pressure ($\Delta p/p_0 < 2\%$), during the initial stage of the flame expansion, and to achieve this aim, all measurements were limited to smaller flame diameters (<50 mm), the total volume of burned gases being under 1.6% of the entire chamber volume. Experimental data used in the analyses were limited to those for which experimental recorded images of the flames were available to insure that cellular instabilities had not occurred.

The flame front images were acquired by the shadowgraph technique. A continuous Ar-Ion laser (Stabilite 2017) and two plano-convex lenses ($f_1 = 25$ mm, $f_2 = 1000$ mm) were combined to create a parallel light beam that crossed the combustion vessel, eventually impacting on a transparent screen. The resulting shadowgrams were recorded with a high speed CMOS camera (Photron APX) operating in a frequency range of 6000–20,000 fps with an exposure time of 20 μs. The spatial resolution was close to 136 μm for all cases. A schematic representation of the experimental layout is given in Ref. [44].

Raw flame images were processed as described in [45] to yield the temporal flame radius evolutions. The optimization procedure developed in [36] based on an integrated form of Eq. (4) (see [35]) was used to extract both s_b^0 and L_b. Unstretched burning velocities were then deduced as $s_u^0 = s_b^0/\sigma$, where σ was numerically evaluated (see the following section). As experimental runs were performed at least twice, s_b^0 and L_b

averages and the corresponding standard deviations are systematically reported.

3. Numerical approach

3.1. Laminar burning velocities

Calculations of burned Markstein lengths require unstretched burning velocities to be computed. These were generated using the Chemkin PREMIX code [46] and associated subroutines [47,48]. Details about the selected kinetic mechanisms [49–51] and simulation conditions are summarized in Table 2. All calculations were performed with the original transport and thermodynamics data provided in refs [49–51]. Multi-component diffusion and thermal diffusion (Soret effect) were enabled for all cases. The PREMIX continuation option was used to successively enlarge the computational domain and refine the solution mesh. The final grids were set so that both laminar burning velocity s_u^0 and flame adiabatic temperature T_b^0 did not show any significant evolution with further refinements. A convergence analysis showed that absolute differences between the present results and those obtained for highly resolved computations ($N_{max} \sim 1000$ pts) did not exceed 2.3 cm s^{-1} for s_u^0 and 24 K for T_b^0 (see $\Delta S_L max$ and $\Delta T_b^0 max$ in Table 2).

3.2. Flame property calculations

The leading flame parameters appearing in Eq. (5) were determined as follows:

- The mixture Lewis numbers *Le* were calculated using the effective formulations Le_H, Le_V and Le_D (see Table 1). Lewis numbers characterizing mixtures with a single fuel "i", were expressed as:

$$Le_i = \frac{D_T}{D_{i/N_2}} \tag{6}$$

with D_T, the mixture thermal diffusivity and D_{i/N_2}, the mass diffusivity of the deficient fuel species "i", conventionally taken as the reactant-inert binary diffusion coefficient. The mixture thermal diffusivity was calculated as:

$$D_T = \frac{\lambda}{\rho_u c_p} \tag{7}$$

with ρ_u, the unburned mixture density, λ and c_p being the mixture-averaged thermal conductivity and specific heat respectively. λ was determined following Mathur et al.'s recommendation [52]:

$$\lambda = \frac{1}{2}\left(\sum_{k=1}^{N} X_k\lambda_k + \frac{1}{\sum_{k=1}^{N}\frac{X_k}{\lambda_k}}\right) \tag{8}$$

N being the total number of species in the mixture, X_k and λ_k, the mole fraction and thermal conductivity of the k^{th} species, respectively. c_p was evaluated using the following mass fraction-weighted formulation:

$$c_p = \sum_{k=1}^{N} c_{p,k}Y_k \tag{9}$$

with Y_k and $c_{p,k}$, the mass fraction and specific heat of the k^{th} species, respectively. Lewis number-related quantities were calculated for the unburned gas temperatures reported in Table 2. A temperature sensitivity analysis showed that the Lewis numbers Le_i's weakly depend on the isotherm at which they are determined. A re-evaluation of the related properties at a higher isotherm, e.g., 1000 K, would achieve a maximum Le_i reduction of 12.4% (iso-octane case). This modification would in turn minimally affect the corresponding Markstein lengths, roughly leading to a downward translation of the L_b curves (maximum averaged decay on the order of 0.13, 0.23, 0.10, 0.05 and 0.09 mm for the H_2/CH_4, H_2/C_3H_8, H_2/C_8H_{18}, H_2/CO {$\varphi = 0.8$ and 0.6} cases respectively). Since the qualitative evolutions of the L_b's are therefore unchanged, the discussion in Section 4 would still be relevant.

To take the influence of the excess reactant (i.e. the oxidizer O_2) into account, an alternate overall effective Lewis number formulation was investigated. This formulation is a weighted average of the Lewis numbers of the "two" reactants (fuel blend/oxidizer), as described by Addabbo et al. in [53]:

$$Le_{X/O_2} = 1 + \frac{(Le_{O_2} - 1) + (Le_X - 1)A}{1 + A} \tag{10}$$

where X denotes the chosen effective formulation H, V or D (see Table 1), Le_{O_2}, the mixture Lewis number based on the O_2 species, and $A = 1 + Ze(1/\varphi - 1)$, the "mixture strength" where φ is the mixture equivalence ratio. A detailed comparison of the Markstein length predictions with and without the O_2 weight reveals that the use of Eq. (10) worsens the observed

Table 2 – Kinetic mechanism characteristics and simulation conditions (all calculations at $p = 1$ atm).

Fuel	Mech. [Ref.] – spec./reac.	φ	T_u (K)	$\Delta S_L max$ (cm s^{-1}) – %	$\Delta T_b^0 max$ (K) – %
H_2/CH_4	GRI Mech. 3.0[a] [49] – 53/325	0.8	298	0.7–0.5	6–0.3
H_2/C_3H_8		0.6		0.9–1.3	7–0.4
H_2/C_8H_{18}	Chaos et al. [50] – 107/723	0.8	423	2.3–1.7	22–1
H_2/CO	Li et al. [51] – 21/84	0.8	297	1.1–0.8	24–1.1
		0.6		0.7–0.9	6–0.3

a Although not recommended for pure propane combustion, Ref. [49] has been selected to model H_2/C_3H_8 lean combustion based on a comparative approach (not detailed here) using different mechanisms. The use of more refined chemical kinetics was not found to affect the qualitative trends presented in this paper.

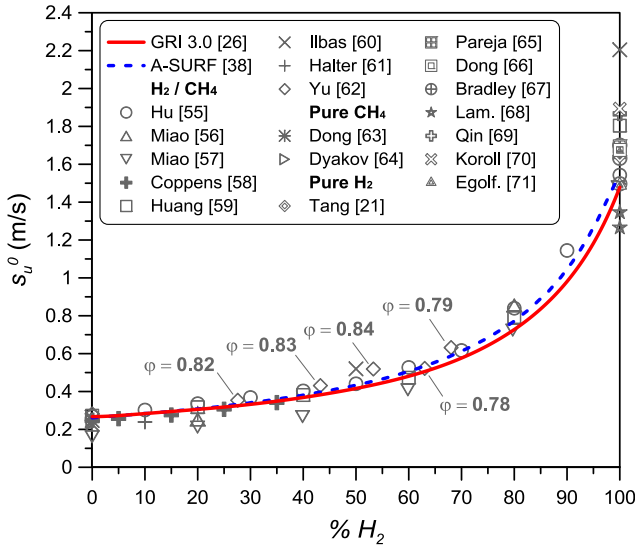

Fig. 2 – Laminar burning velocities of H_2/CH_4/air flames versus H_2 fuel volumetric content (φ = 0.8, T_u = 298 K).

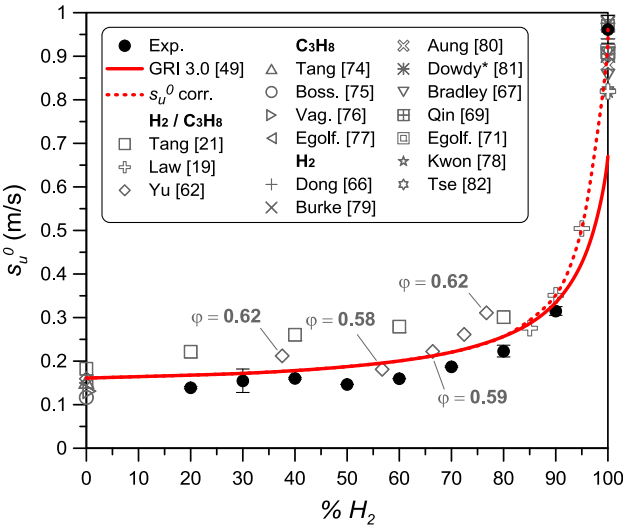

Fig. 4 – Laminar burning velocities of H_2/C_3H_8/air flames versus H_2 fuel volumetric content (φ = 0.6, T_u = 298 K, *experiments at φ = 0.62). The velocity correction (red-dotted line) is performed by applying a spline smoothing function on the data points of Ref. [19] (85–95% H_2 range) and the present 100% H_2 data point combined. (For interpretation of the references to colour in this figure legend, the reader is referred to the web version of this article.)

agreements with the experimental results (see Section 4), especially for the lightest fuels (CH_4, CO) and the highest H_2 contents. For the sake of completeness, burned Markstein lengths calculated with Le_{H/O_2}, Le_{V/O_2} and Le_{D/O_2} are reported in the present work (see dotted lines in Figs. 3, 5, 7, 10 and 11) but, given the inconclusive trends, will not be further commented on in the remaining sections.

- The flame Zel'dovich numbers were calculated as:

$$Ze = \frac{E_a\left(T_b^0 - T_u\right)}{RT_b^{02}} \tag{11}$$

with E_a, the overall activation energy and R, the universal gas constant. For sufficiently off-stoichiometric mixtures, E_a can be retrieved from the analysis of the laminar burning rate sensitivity to the adiabatic flame temperature variation [10,54]:

$$E_a = -2R\left[\frac{\partial\left(\ln \rho_u s_u^0\right)}{\partial\left(1/T_b^0\right)}\right]_p \tag{12}$$

where p is the pressure. In the present case, this sensitivity was numerically captured by varying the amount of inert species (N_2) at fixed fuel composition and equivalence ratio.

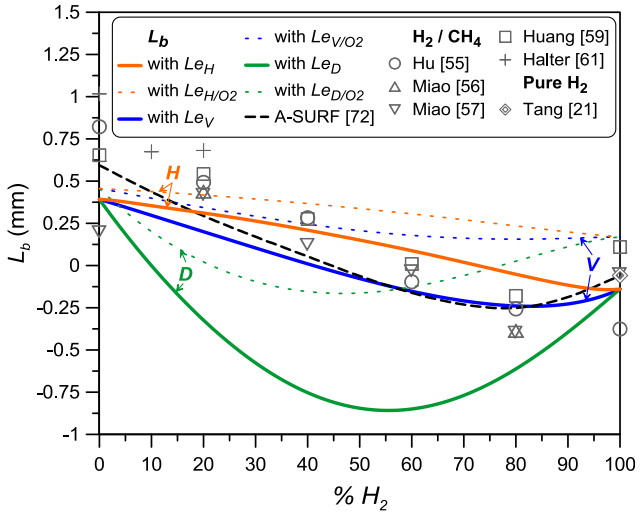

Fig. 3 – H_2/CH_4/air Markstein length versus H_2 fuel volumetric content (φ = 0.8, T_u = 298 K).

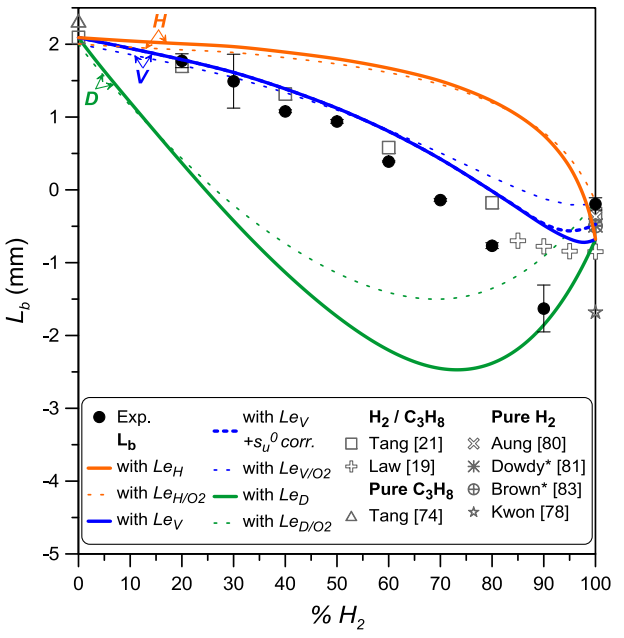

Fig. 5 – H_2/C_3H_8/air Markstein length versus H_2 fuel volumetric content (φ = 0.6, T_u = 298 K, *experiments at φ = 0.62).

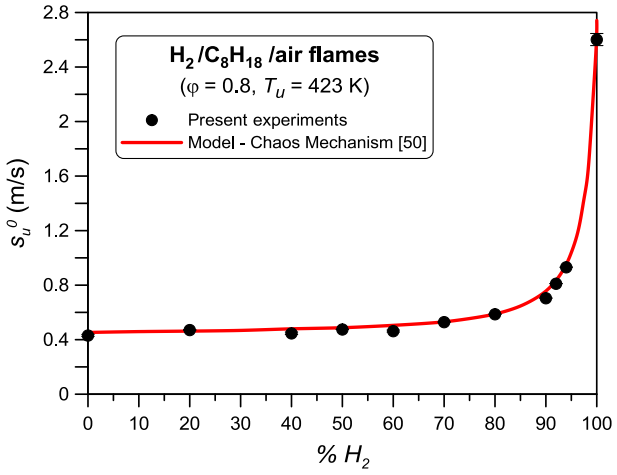

Fig. 6 – Laminar burning velocity of H_2/C_8H_{18}/air flames versus H_2 fuel volumetric content.

- Assuming chemical equilibrium, the flame thermal expansion coefficients were conventionally calculated as the unburned to burned gas density ratio, i.e.:

$$\sigma = \rho_u/\rho_b \tag{13}$$

- The flame thicknesses were evaluated through the diffusion scaling approach:

$$\delta = D_T/s_u^0 \tag{14}$$

where D_T is evaluated according to Eq. (7).

The flame characteristics (s_u^0, ρ_u, ρ_b, T_b^0) were obtained as part of the solution of the PREMIX computations. Pure species transport and thermodynamic properties were calculated by a polynomial fitting formula whose coefficients were respectively: (i) computed by the PREMIX transport subroutine [48], (ii) taken from the mechanisms thermodynamic inputs,

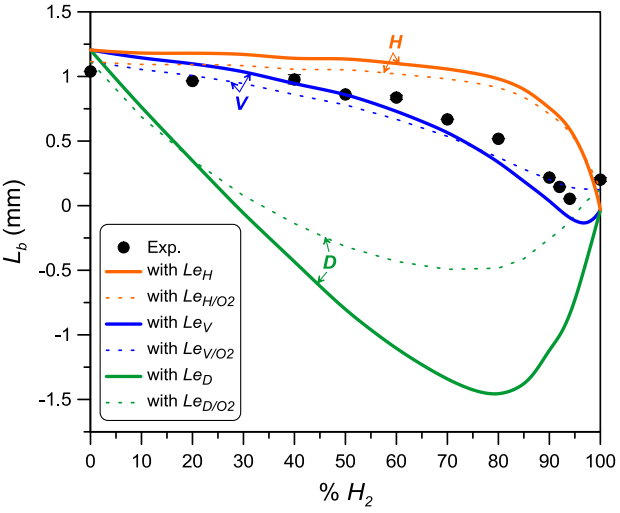

Fig. 7 – H_2/C_8H_{18}/air Markstein length versus H_2 fuel volumetric content (φ = 0.8, T_u = 423 K).

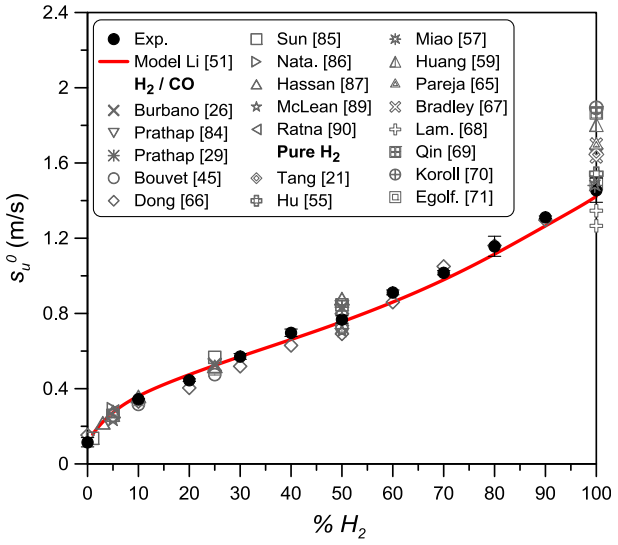

Fig. 8 – Laminar burning velocities of H_2/CO/air flames versus H_2 fuel volumetric content (φ = 0.8, T_u = 297 K).

respectively. All the afore-introduced definitions are consistent with the approach detailed in [38] that led to Eqs. (4) and (5). Note here however that σ is the reciprocal of the thermal expansion coefficient as introduced in [37–39].

4. Results and discussion

4.1. *Methane flames*

Calculated laminar burning velocities and Markstein lengths of H_2/CH_4/air mixtures are respectively shown in Figs. 2 and 3 along with the literature experimental datasets for H_2/CH_4

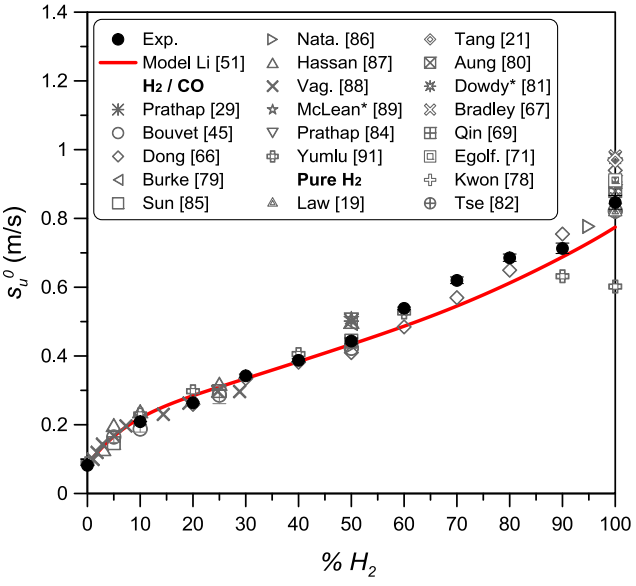

Fig. 9 – Laminar burning velocities of H_2/CO/air flames versus H_2 fuel volumetric content (φ = 0.6, T_u = 297 K, *experiments at φ = 0.62).

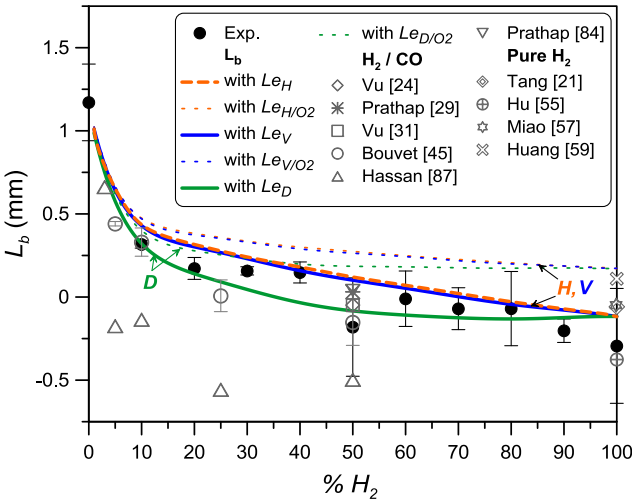

Fig. 10 – H_2/CO/air Markstein length versus H_2 fuel volumetric content (φ = 0.8, T_u = 297 K).

[55–62], pure CH_4 [63,64] and pure H_2 [21,65–71] fuels. It can be seen in Fig. 2 that previous burning velocity measurements for H_2/CH_4 blends are rather scarce for hydrogen contents above 80%. Reported measurements for pure hydrogen flames show considerable disparities, most values being in the 1.2–1.9 m s^{-1} range. The PREMIX computations with the GRI Mech. 3.0 demonstrate an overall good agreement with the experiments, reaching a flame speed of 1.48 m s^{-1} at 100% of H_2. Also shown are the numerical values extracted from OPF simulations performed by Chen [72] with the one-dimensional code A-SURF, incorporating the GRI Mech. 3.0 chemistry. The two sets of predictions are almost identical, although a minor offset becomes discernible as the hydrogen content is

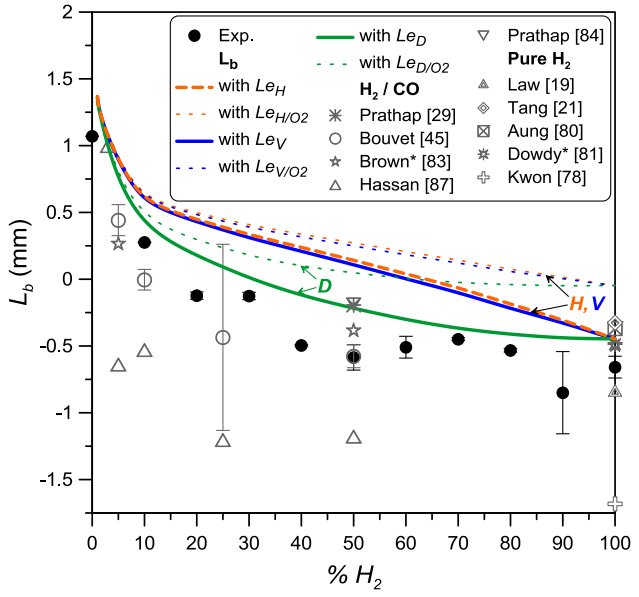

Fig. 11 – H_2/CO/air Markstein length versus H_2 fuel volumetric content (φ = 0.6, T_u = 297 K, *experiments at φ = 0.62).

increased. This might be attributed to the use of linear extrapolation in [72], a procedure known to slightly overestimate unstretched flame speeds for nonequidiffusive mixtures.

Data points of Ref. [55] aside, the experimental Markstein lengths presented in Fig. 3 display a non-monotonic behavior, showing a gradual decrease up to 80% of H_2, followed by a noticeable increase towards the pure H_2 case. This "re-stabilization" trend was previously reported by Law and Kwon [19] for lean (φ = 0.6) and stoichiometric H_2/CH_4 flames. A similar observation was made by Sankaran and Im for their 1D computations of lean H_2/CH_4 opposed jet flames [73]. A later study by Chen [72] showed that the non-monotonic evolution of L_b is a general stability feature of H_2/CH_4/air flames. This behavior is qualitatively well captured by Eq. (5) combined with Le_V. In this case, both Markstein length sign (~41% H_2) and slope (~83% H_2) inversions compare well with the 1D computations of Chen [72]. The analytical form seems however to slightly underestimate experimental Markstein lengths at lower H_2 contents. The use of Eq. (1) or (3) worsens the overall qualitative agreement with the experiments.

4.2. *Propane flames*

Figs. 4 and 5 show both measured and calculated laminar flame speeds and burned Markstein lengths for the H_2/C_3H_8/air blends of interest. Previously published measurements for H_2/C_3H_8 [19,21,62], pure C_3H_8 [74–77] and pure H_2 [66,67,69,71,78–83] fuels are reported as well. The laminar burning velocity predictions with the GRI Mech. 3.0 find a good agreement with the present measurements up to 90% of H_2. Above this proportion, the mechanism clearly underestimates experimental values, predicting an H_2/air flame speed of 0.67 m s^{-1}, whereas measurements cluster in the 0.8–1.0 m s^{-1} interval.

While all Markstein length measurements confirm the gradual destabilizing effect of H_2 addition in C_3H_8 (see Fig. 5), the present experiment suggests that a marked slope inversion occurs around 90% of H_2, followed by a sharp L_b increase. Akin to the methane cases, the analytical results show that the Le_V formulation provides the best qualitative match overall. The close quantitative agreement with the results reported by Tang et al. [21] and Law and Kwon [19] should also be underlined. Although it may not be discernible on Fig. 5, Eq. (5) combined with Le_V actually predicts, to a lesser extent, the slope inversion that is seen experimentally. The latter becomes evident if the computed burning velocities are corrected to match the available measurements in the 90–100% H_2 range (see s_u^0corr. in Figs. 4 and 5).

4.3. *Iso-octane flames*

As seen in Fig. 6, the computations performed with the mechanism of Chaos et al. [50] closely agree with the experimental observations. The burning velocity of the H_2/C_8H_{18}/air flames stays mostly unchanged in the first 60% of H_2 addition, increases moderately in the 60–85% range to finally end with a "burst" (~2 m s^{-1}) in the last 15%.

The corresponding Markstein lengths shown in Fig. 7 demonstrate that the Le_V model outperforms both Le_H and

Le_D formulations. While a proper decreasing trend for L_b is recovered using Le_V, the analytical form also accurately predicts the slope inversion occurring around 95% of H_2 addition. Both Le_H and Le_D approaches lead to L_b evolutions that are distinctly incompatible with the experimental trends.

4.4. *Syngas flames*

The laminar burning velocities and burned Markstein lengths of the H_2/CO/air blends of interest (φ = 0.8 and 0.6) are respectively reported in Figs. 8–11. The literature datasets for H_2/CO [24,26,29,31,45,66,79,83–91] and pure H_2 [19,21,55,57,59,65,67–71,78,80–82] fuels are included as well. Measured velocities for both equivalence ratios reveal that the 55–95% H_2 range has not been extensively studied as compared to the lower H_2 content cases (see Figs. 8 and 9). Both velocity increases with H_2 addition are very well predicted by the mechanism of Li et al. [51], including the well known non-linear behavior at higher carbon monoxide contents (%H_2 < 10%). A slight model underestimation of about 7 cm s^{-1} should be mentioned for the higher H_2 content mixtures (%H_2 > 60) at φ = 0.6.

The burned Markstein lengths for φ = 0.8 are shown in Fig. 10. The measurements indicate a strong destabilization effect of the H_2 addition in CO (%H_2 < 10%), followed by a moderate linear decrease of L_b up to the pure H_2 case. This behavior is particularly well reproduced by the analytical model incorporating either Le_H or Le_V. Note here that for syngas flames, the collapse of the Le_H and Le_V approaches is not surprising since the heat of combustion per unit mass of hydrogen is nearly 12 times that of carbon monoxide.[3] The predominance of the hydrogen heat release results in a quasi-linear weighting of the respective Le_i's. Given the weak sensitivity of Eq. (5) to Le_{eff} and the level of the reported experimental uncertainties, a clear discrimination of the relevant approach(es) (Le_H/Le_V vs. Le_D) is not possible. This issue can be overcome by considering leaner cases. The measured Markstein lengths presented in Fig. 11 for the equivalence ratio 0.6 show a significant deviation from the Le_H/Le_V-based models. In fact, the observed adequacy with the diffusion-based approach suggests that hydrogen has an overwhelming effect on carbon monoxide regarding the syngas flame stability, as compared to other H_2/HC blends. Additional insights can be gained if the unburned fuel species evolutions are compared for all the studied fuels as the flame front is crossed. This has been performed in Fig. 12 for a fixed unburned fuel composition (50/50% H_2/HC) and equivalence ratio (φ = 0.6). Unlike conventional H_2/HC blends, the H_2/CO proportion is found to vary strongly throughout the flame and a significant H_2 depletion is recorded in this particular case. While this observation corroborates the dominant effect of hydrogen on the syngas flame stability, it also suggests that the latter is influenced by the detailed chemical processes arising in the reactive front. For syngas flames, the strong kinetic coupling between the hydrogen and carbon monoxide chemistry (H_2 as a unique source of H atoms for radical pool build-up) clearly goes beyond the single step chemistry assumption involved in the derivation of Eq. (5). As such, a straightforward identification of the appropriate Le_{eff} formulation seems to be compromised.

[3] Against 2–3 times for the afore-tested alkanes.

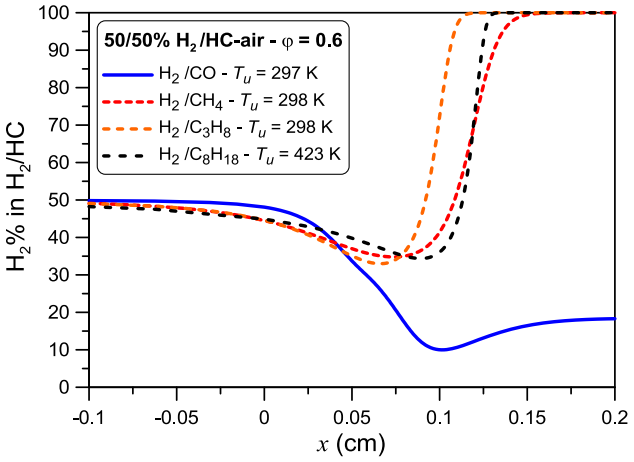

Fig. 12 – Comparison of the fuel composition evolutions throughout the flame fronts.

4.5. Le_{eff} *models and the burned Markstein length slope inversion*

A mechanistic interpretation of the respective performances of the different Lewis number formulations is excluded since detailed transport processes should be scrutinized on the molecular level to yield further explanations. We can note, however, that:

i The use of two distinct Le_i's to shape any Le_{eff} formulation conceptually pre-supposes, as schematically shown in Fig. 13, that each fuel reacts individually. This underlying assumption being recognized, a Le_i weighting depending on the respective number of fuel entities, i.e. the fuel volumetric contents, follows quite naturally. In this context, the superiority of the Le_V formulation should be of no surprise.

ii The heat release formulation Le_H seems to over-weight the hydrocarbon influence on the H_2/HC flame stability characteristics. Although the heat of combustion per mass of hydrogen is 2–3 times higher than that of the

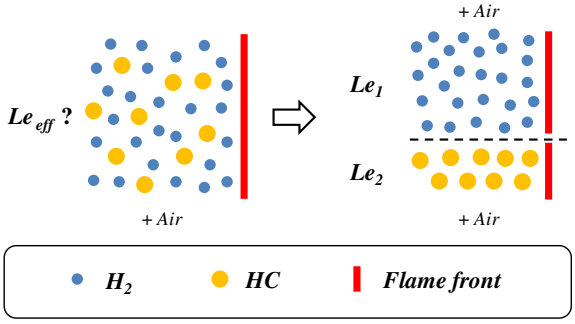

Fig. 13 – Schematic representation of the underlying assumption of two fuel Lewis numbers Le_i for the elaboration of a Le_{eff} approach.

alkanes, the tremendous difference in the molecular masses of the two fuels delays the hydrogen addition effects to the higher H_2 contents.

iii The diffusion formulation Le_D is found to clearly overweight the hydrogen influence on the H_2/HC flame stability characteristics. This trend shows that Eq. (3), which encapsulates the hypothesis of a highly curved flame through the leading edge concept [14], is not of broad applicability.

The demonstrated adequacy of the Le_V model allows for a more detailed interpretation of the Markstein length non-monotonic behavior observed for the hydrogen/alkane fuel blends. Normalizing Eq. (5) by δ, hence yielding the Markstein number expression, and further differentiating with respect to the hydrogen percent in the fuel blend leads to:

$$\partial_{H_2}(M_b) = A_1\partial_{H_2}(Le) + A_2\partial_{H_2}(Ze) + A_3\partial_{H_2}(\sigma) \quad (15)$$

with

$$A_1 = \left(\frac{\sigma}{Le^2}\right)\left(\frac{Ze}{2} - 1\right) \quad (16)$$

$$A_2 = -\left(\frac{\sigma}{2}\right)\left(\frac{1}{Le} - 1\right) \quad (17)$$

$$A_3 = \left[\left(\frac{1}{Le}\right) - \left(\frac{Ze}{2}\right)\left(\frac{1}{Le} - 1\right)\right] \quad (18)$$

It is seen that the M_b variation is governed by the respective variations of Le, Ze and σ, which are themselves weighted by the non-linear coefficients A_i's. To enlighten the discussion, the different terms of Eq. (15) are evaluated and compared in Fig. 14 for the hydrogen/methane flame case. It is found in Fig. 14a that the sign of $\partial_{H_2}(M_b)$ depends on the respective contributions of the first two terms (T_1, T_2) in the RHS of Eq. (15). While T_1 is always negative because of the opposite signs of A_1 and $\partial_{H_2}(Le)$, its evolution with H_2 addition is set only by A_1 since, by definition, $\partial_{H_2}(Le)$ is constant. Fig. 14b shows that A_1 progressively increases up to 90% of H_2, followed by a short decrease towards the pure H_2 case. Eq. (16) reveals that this change is a result of the counteracting effects of the progressive Le decrease versus Ze late decrease as the H_2 content is raised. On the other hand, T_2 is always positive due to the negative signs of both A_2 and $\partial_{H_2}(Ze)$. Given that A_2 varies moderately varying over the entire H_2 range, the exponential increase of T_2 can be directly attributed to the steep $\partial_{H_2}(Ze)$ decrease observed in Fig. 14c. The former is found to progressively overcome the destabilizing effect of Le and ultimately leads to the M_b slope inversion (see Fig. 14a). The results obtained in the present investigation suggest that this stability trade-off is common among hydrogen/alkane fuel blends. We finally note that the demonstration detailed above is in line with the qualitative discussion given by Sankaran and Im [73] regarding the stability characteristics of lean hydrogen/methane counterflow flames.

4.6. *Concluding remarks*

We conclude the discussion by pointing out that a perfect quantitative match between both analytical and experimental burned Markstein lengths should not be expected for several reasons. An important reason is the potential inaccuracy of the chosen kinetic mechanisms in reproducing both laminar flame speeds and flame burning rate sensitivity to dilution. Although the kinetic mechanisms were selected for their comprehensive development against large sets of experimental conditions, the wide fuel composition ranges investigated in the present study are clearly demanding, and set new ways for mechanism improvements. The simplifying assumptions involved in the derivation of Eq. (5) (e.g., constant density model, flame thickness based on the diffusion scaling approach) should also be mentioned as sources of potential inaccuracy. Although revisiting these core hypotheses clearly goes beyond the scope of the present work, we shall however recall that the validity of Eq. (5) was confirmed through detailed numerical simulations in the work of Chen et al. [37,38], in turn ensuring that Eq. (5) captures the fundamental physics ruling the flame propagation. We also note that the agreement between both experimental and calculated Markstein lengths for pure fuel mixtures is of prime importance. Given the functional form of Eq. (5), this agreement is a strong sign of model consistency regarding the choice of the flame thickness definition.

Keeping these issues in mind, it should be recognized that the level of agreement found for the alkanes (methane, propane and iso-octane) is remarkable. It is believed that the ability of the Le_V-based approach to reproduce salient

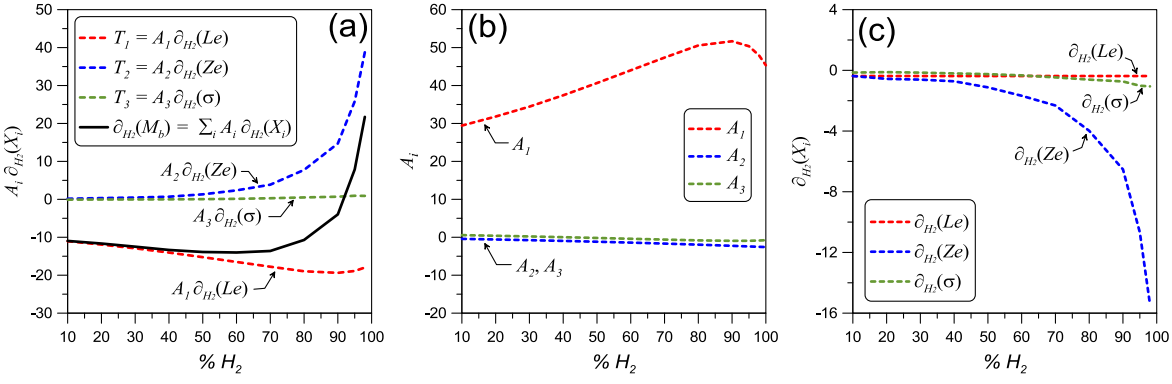

Fig. 14 – Evaluation of the terms of Eq. (15) for the hydrogen/methane case: comparison of the (a) $A_i\partial_{H_2}(X_i)$'s, (b) A_i's and (c) $\partial_{H_2}(X_i)$'s.

characteristics such as Markstein length sign and slope inversions provides engaging elements for future studies. We also note, as underlined by Chen et al. in [37,39], that Eq. (5) is similar to Markstein length expressions derived for premixed counterflow flames using flame integral analysis (cf. Law [10]), in turn suggesting that the present results are of broad applicability. To substantiate this fact, additional investigations using different experimental apparatuses would be required. Counterflow flames would particularly suit this need because stretched effects acting on the flame can be easily quantified. Provided that a proper reference location is chosen within the reactive front, theoretical formulations describing the flame propagation are available (e.g. Tien and Matalon [92]) and could be used along with the associated experiments to confirm the universality of the current results.

5. Conclusion

Effective Lewis number formulations for lean premixed hydrogen/hydrocarbon/air mixtures have been investigated in the framework of an existing outwardly propagating flame theory. To do so, laminar burning velocities and burned Markstein lengths of H_2/CH_4, H_2/C_3H_8, H_2/C_8H_{18} and H_2/CO fuel blends in air were experimentally and numerically determined for a wide range of fuel compositions (0/100% → 100/0% H_2/HC). The following conclusions are of particular importance:

- The volumetric weighted approach $Le_V = x_1Le_1+x_2Le_2$ was found to be the most consistent one for the tested alkanes (CH_4, C_3H_8 and C_8H_{18}), leading to a qualitatively accurate prediction of both Markstein length sign and slope inversions. This formulation should be preferred when commenting on lean H_2/HC/air flame stability.
- The stabilizing effect of hydrogen additions in highly hydrogenated H_2/HC/air blends has been confirmed for all the alkanes tested, thereby extending early observations made for H_2/CH_4/air flames. This Markstein length non-monotonic behavior is the result of the counteracting effects of *Le* (destabilization) versus *Ze* (stabilization) reduction as the mixture hydrogen content is increased. This trend was not recorded for syngas flames.
- The relevance of the Le_V formulation could not be confirmed for syngas mixtures. In this case, the Markstein length and therefore flame stability are expected to be influenced by detailed chemical effects that cannot be taken into account in classical one-step chemistry models. Results show however that hydrogen has an overwhelming effect on carbon monoxide as compared to other hydrogen/hydrocarbon blends investigated.

Acknowledgements

This work was supported by the Mid-career Researcher Program through an NRF grant funded by the MEST (2011-0016455), contracted through the IAAT at Seoul National University and the New & Renewable Energy Technology Development Program (No. 2011951010001C) of the KETEP grant funded by the MKE.

REFERENCES

[1] Lewis WK. The evaporation of a liquid into a gas. Trans Am Soc Mech Eng 1922;44:325–40.
[2] Webb RL. Standard nomenclature for mass transfer processes. Int Com Heat Mass Transfer 1990;17:529–35.
[3] Wu CK, Law CK. On the determination of laminar flame speeds from stretched flames. Proc Combust Inst 1985;20:1941–9.
[4] Ishizuka S, Law CK. Experimental study on extinction and stability of stretched premixed flames. Proc Combust Inst 1982;19:327–35.
[5] Sato Ji. Effects of Lewis number on extinction behaviour of premixed flames in a stagnation flow. Proc Combust Inst 1982;19:1541–8.
[6] Law CK, Ishizuka S, Cho P. On the opening of premixed Bunsen flame tips. Combust Sci Technol 1982;28:89–96.
[7] Sivashinsky GI. On a distorted flame front as a hydrodynamic discontinuity. Acta Astronautica 1976;3:889–918.
[8] Matalon M. On flame stretch. Combust Sci Technol 1983;31:169–81.
[9] Clavin P. Dynamic behavior of premixed flame fronts in laminar and turbulent flows. Prog Energy Combust Sci 1985;11:1–59.
[10] Law CK. Combustion physics. New York: Cambridge University Press; 2006.
[11] Wu MS, Kwon S, Driscoll JF, Faeth GM. Turbulent premixed hydrogen/air flames at high Reynolds numbers. Combust Sci Technol 1990;73:327–50.
[12] Abdel-Gayed RG, Bradley D, Hamid MN, Lawes M. Lewis number effects on turbulent burning velocity. Proc Combust Inst 1985;20:505–12.
[13] Bradley D. How fast can we burn? Proc Combust Inst 1992;24:247–62.
[14] Dinkelacker F, Manickam B, Muppala SPR. Modelling and simulation of lean premixed turbulent methane/hydrogen/air flames with an effective Lewis number approach. Combust Flame 2011;158:1742–9.
[15] Chen JB, Im HG. Stretch effects on the burning velocity of turbulent premixed hydrogen/air flames. Proc Combust Inst 2000;28:211–8.
[16] Bell JB, Cheng RK, Day MS, Shepherd IG. Numerical simulation of Lewis number effects on lean premixed turbulent flames. Proc Combust Inst 2007;31:1309–17.
[17] Bell SR, Gupta M. Extension of the lean operating limit for natural gas fueling of a spark ignited engine using hydrogen blending. Combust Sci Technol 1997;123:23–48.
[18] Frenillot JP, Cabot G, Cazalens M, Renou B, Boukhalfa MA. Impact of H_2 addition on flame stability and pollutant emissions for an atmospheric kerosene/air swirled flame of laboratory scaled gas turbine. Int J Hydrogen Energy 2009;34:3930–44.
[19] Law CK, Kwon OC. Effects of hydrocarbon substitution on atmospheric hydrogen-air flame propagation. Int J Hydrogen Energy 2004;29:867–79.
[20] Law CK, Jomaas G, Bechtold JK. Cellular instabilities of expanding hydrogen/propane spherical flames at elevated pressures: theory and experiment. Proc Combust Inst 2005;30:159–67.
[21] Tang C, Huang Z, Jin C, He J, Wang J, Wang X, et al. Laminar burning velocities and combustion characteristics of propane-hydrogen-air premixed flames. Int J Hydrogen Energy 2008;33:4906–14.

[22] Tang C, Huang Z, Wang J, Zheng J. Effects of hydrogen addition on cellular instabilities of the spherically expanding propane flames. Int J Hydrogen Energy 2009;34:2483–7.
[23] Hu E, Huang Z, He J, Zheng J, Miao H. Measurements of laminar burning velocities and onset of cellular instabilities of methane–hydrogen–air flames at elevated pressures and temperatures. Int J Hydrogen Energy 2009;34:5574–84.
[24] Vu TM, Park J, Kwon OB, Bae DS, Yun JH, Keel SI. Effects of diluents on cellular instabilities in outwardly propagating spherical syngas-air premixed flames. Int J Hydrogen Energy 2010;35:3868–80.
[25] Tang CL, Huang ZH, Law CK. Determination, correlation, and mechanistic interpretation of effects of hydrogen addition on laminar flame speeds of hydrocarbon–air mixtures. Proc Combust Inst 2011;33:921–8.
[26] Burbano HJ, Pareja J, Amell AA. Laminar burning velocities and flame stability analysis of H_2/CO/air mixtures with dilution of N_2 and CO_2. Int J Hydrogen Energy 2011;36:3232–42.
[27] Liu CC, Shy SS, Chiu CW, Peng MW, Chung HJ. Hydrogen/carbon monoxide syngas burning rates measurements in high-pressure quiescent and turbulent environment. Int J Hydrogen Energy 2011;36:8595–603.
[28] Wu F, Kelley AP, Tang C, Zhu D, Law CK. Measurement and correlation of laminar flame speeds of CO and C2 hydrocarbons with hydrogen addition at atmospheric and elevated pressures. Int J Hydrogen Energy 2011;36:13171–80.
[29] Prathap C, Ray A, Ravi MR. Effects of dilution with carbon dioxide on the laminar burning velocity and flame stability of H_2–CO mixtures at atmospheric condition. Combust Flame 2012;159:482–92.
[30] Vu TM, Park J, Kwon OB, Kim JS. Effects of hydrocarbon addition on cellular instabilities in expanding syngas-air spherical premixed flames. Int J Hydrogen Energy 2009;34:6961–9.
[31] Vu TM, Park J, Kim JS, Kwon OB, Yun JH, Keel SI. Experimental study on cellular instabilities in hydrocarbon/hydrogen/carbon monoxide-air premixed flames. Int J Hydrogen Energy 2011;36:6914–24.
[32] Muppala SPR, Nakahara M, Aluri NK, Kido H, Wen JX, Papalexandris MV. Experimental and analytical investigation of the turbulent burning velocity of two-component fuel mixtures of hydrogen, methane and propane. Int J Hydrogen Energy 2009;34:9258–65.
[33] Muppala SPR, Aluri NK, Dinkelacker F, Leipertz A. Development of an algebraic reaction rate closure for the numerical calculation of turbulent premixed methane, ethylene, and propane/air flames for pressures up to 1.0 MPa. Combust Flame 2005;140:257–66.
[34] Dinkelacker F. Why the Lewis number seems to have an unexpected importance even in highly turbulent flames!. In: 11th International workshop on premixed turbulent flames. Montreal, Canada: McGill University; 2008.
[35] Kelley AP, Law CK. Nonlinear effects in the extraction of laminar flame speeds from expanding spherical flames. Combust Flame 2009;156:1844–51.
[36] Halter F, Tahtouh T, Mounaïm-Rousselle C. Nonlinear effects of stretch on the flame front propagation. Combust Flame 2010;157:1825–32.
[37] Chen Z. On the extraction of laminar flame speed and Markstein length from outwardly propagating spherical flames. Combust Flame 2011;158:291–300.
[38] Chen Z, Ju Y. Theoretical analysis of the evolution from ignition kernel to flame ball and planar flame. Combust Theory Model 2007;11:427–53.
[39] Chen Z, Burke MP, Ju Y. Effects of Lewis number and ignition energy on the determination of laminar flame speed using propagating spherical flames. Proc Combust Inst 2009;32:1253–60.
[40] Ronney PD, Sivashinsky GI. A theoretical study of propagation and extinction of nonsteady spherical flame fronts. SIAM J Appl Math 1989;49:1029–46.
[41] Sun CJ, Sung CJ, Zhu DL, Law CK. Response of counterflow premixed and diffusion flames to strain rate variations at reduced and elevated pressures. Proc Combust Inst 1996;26:1111–20.
[42] Sun CJ, Sung CJ, He L, Law CK. Dynamics of weakly stretched flames: quantitative description and extraction of global flame parameters. Combust Flame 1999;118:108–28.
[43] Jomaas G, Law CK, Bechtold JK. On transition to cellularity in expanding spherical flames. J Fluid Mech 2007;583:1–26.
[44] Togbe C, Dagaut P, Halter F, Foucher F. 2-Propanol oxidation in a pressurized jet-stirred reactor (JSR) and combustion bomb: experimental and detailed kinetic modeling study. Energy Fuels 2011;25:676–83.
[45] Bouvet N, Chauveau C, Gökalp I, Halter F. Experimental studies of the fundamental flame speeds of syngas (H_2/CO)/air mixtures. Proc Combust Inst 2011;33:913–20.
[46] Kee RJ, Grcar JF, Smooke MD, Miller JA. A Fortran program for modeling steady laminar one-dimensional premixed flames, report SAND85-8240. Livermore, CA: Sandia National Laboratories; 1985.
[47] Kee RJ, Rupley FM, Miller JA. Chemkin-II: a fortran chemical kinetics package for the analysis of gas phase chemical kinetics. Sandia Report SAND89-8009B 1989.
[48] Kee RJ, Dixon-Lewis G, Warnatz J, Coltrin RE, Miller JA. A Fortran computer package for the evaluation of gas-phase, multicomponent transport properties. SAND86-8246. Sandia National Laboratory; 1986.
[49] Smith GP, Golden DM, Frenklach M, Moriarty NW, Eiteneer B, Goldenberg M, et al. GRI Mech. 3.0; 2006. Available from: http://www.meberkeleyedu/gri_mech/.
[50] Chaos M, Kazakov A, Zhao Z, Dryer FL. A high-temperature chemical kinetic model for primary reference fuels. Int J Chem Kinet 2007;39:399–414.
[51] Li J, Zhao Z, Kazakov A, Chaos M, Dryer FL, Scire JJ. A comprehensive kinetic mechanism for CO, CH_2O, and CH_3OH combustion. Int J Chem Kinet 2007;39:109–36.
[52] Mathur S, Tondon PK, Saxena SC. Thermal conductivity of binary, ternary and quaternary mixtures of rare gases. Mol Phys 1967;12:569–79.
[53] Addabbo R, Bechtold JK, Matalon M. Wrinkling of spherically expanding flames. Proc Combust Inst 2002;29:1527–35.
[54] Egolfopoulos FN, Law CK. Chain mechanisms in the overall reaction orders in laminar flame propagation. Combust Flame 1990;80:7–16.
[55] Hu E, Huang Z, He J, Jin C, Zheng J. Experimental and numerical study on laminar burning characteristics of premixed methane–hydrogen–air flames. Int J Hydrogen Energy 2009;34:4876–88.
[56] Miao H, Jiao Q, Huang Z, Jiang D. Measurement of laminar burning velocities and Markstein lengths of diluted hydrogen-enriched natural gas. Int J Hydrogen Energy 2009;34:507–18.
[57] Miao H, Jiao Q, Huang Z, Jiang D. Effect of initial pressure on laminar combustion characteristics of hydrogen enriched natural gas. Int J Hydrogen Energy 2008;33:3876–85.
[58] Coppens FHV, De Ruyck J, Konnov AA. Effects of hydrogen enrichment on adiabatic burning velocity and NO formation in methane + air flames. Exp Thermal Fluid Sci 2007;31:437–44.
[59] Huang Z, Zhang Y, Zeng K, Liu B, Wang Q, Jiang D. Measurements of laminar burning velocities for natural gas–hydrogen–air mixtures. Combust Flame 2006;146:302–11.

[60] Ilbas M, Crayford AP, Yılmaz İ, Bowen PJ, Syred N. Laminar-burning velocities of hydrogen–air and hydrogen–methane–air mixtures: an experimental study. Int J Hydrogen Energy 2006;31:1768–79.
[61] Halter F, Chauveau C, Djebaïli-Chaumeix N, Gökalp I. Characterization of the effects of pressure and hydrogen concentration on laminar burning velocities of methane–hydrogen–air mixtures. Proc Combust Inst 2005;30:201–8.
[62] Yu G, Law CK, Wu CK. Laminar flame speeds of hydrocarbon + air mixtures with hydrogen addition. Combust Flame 1986;63:339–47.
[63] Dong Y, Vagelopoulos CM, Spedding GR, Egolfopoulos FN. Measurement of laminar flame speeds through digital particle image velocimetry: mixtures of methane and ethane with hydrogen, oxygen, nitrogen, and helium. Proc Combust Inst 2002;29:1419–26.
[64] Dyakov IV, Konnov AA, De Ruyck J, Bosschaart KJ, Brock ECM, De Goey LPH. Measurement of adiabatic burning velocity in methane-oxygen-nitrogen mixtures. Combust Sci Technol 2001;172:81–96.
[65] Pareja J, Burbano HJ, Ogami Y. Measurements of the laminar burning velocity of hydrogen-air premixed flames. Int J Hydrogen Energy 2010;35:1812–8.
[66] Dong C, Zhou Q, Zhao Q, Zhang Y, Xu T, Hui S. Experimental study on the laminar flame speed of hydrogen/carbon monoxide/air mixtures. Fuel 2009;88:1858–63.
[67] Bradley D, Lawes M, Liu K, Verhelst S, Woolley R. Laminar burning velocities of lean hydrogen-air mixtures at pressures up to 1.0 MPa. Combust Flame 2007;149:162–72.
[68] Lamoureux N, Djebaïli-Chaumeix N, Paillard CE. Laminar flame velocity determination for H_2–air–He–CO_2 mixtures using the spherical bomb method. Exp Thermal Fluid Sci 2003;27:385–93.
[69] Qin X, Kobayashi H, Niioka T. Laminar burning velocity of hydrogen-air premixed flames at elevated pressure. Exp Thermal Fluid Sci 2000;21:58–63.
[70] Koroll GW, Kumar RK, Bowles EM. Burning velocities of hydrogen-air mixtures. Combust Flame 1993;94:330–40.
[71] Egolfopoulos FN, Law CK. An experimental and computational study of the burning rates of ultra-lean to moderate-rich $H_2/O_2/N_2$ laminar flames with pressure variations. Proc Combust Inst 1991;23:333–40.
[72] Chen Z. Effects of hydrogen addition on the propagation of spherical methane/air flames: a computational study. Int J Hydrogen Energy 2009;34:6558–67.
[73] Sankaran R, Im HG. Effects of hydrogen addition on the Markstein length and flammability limit of stretched methane/air premixed flames. Combust Sci Technol 2006;178:1585–611.
[74] Tang C, Zheng J, Huang Z, Wang J. Study on nitrogen diluted propane-air premixed flames at elevated pressures and temperatures. Energy Conversion Manag 2010;51:288–95.
[75] Bosschaart KJ, Versluis M, Knikker R, Van Der Meer TH, Schreel KRAM, De Goey LPH, et al. The heat flux method for producing burner stabilized adiabatic flames: an evaluation with cars thermometry. Combust Sci Technol 2001;169:69–87.
[76] Vagelopoulos CM, Egolfopoulos FN, Law CK. Further considerations on the determination of laminar flame speeds with the counterflow twin flame technique. Proc Combust Inst 1994;25:1341–7.
[77] Egolfopoulos FN, Zhu DL, Law CK. Experimental and numerical determination of laminar flamespeeds: mixtures of C2-hydrocarbons with oxygen and nitrogen. Proc Combust Inst 1991;23:471–8.
[78] Kwon OC, Faeth GM. Flame/stretch interactions of premixed hydrogen-fueled flames: measurements and predictions. Combust Flame 2001;124:590–610.
[79] Burke MP, Chen Z, Ju Y, Dryer FL. Effect of cylindrical confinement on the determination of laminar flame speeds using outwardly propagating flames. Combust Flame 2009;156:771–9.
[80] Aung KT, Hassan MI, Faeth GM. Flame stretch interactions of laminar premixed hydrogen/air flames at normal temperature and pressure. Combust Flame 1997;109:1–24.
[81] Dowdy DR, Smith DB, Taylor SC, Williams A. The use of expanding spherical flames to determine burning velocities and stretch effects in hydrogen/air mixtures. Proc Combust Inst 1991;23:325–32.
[82] Tse SD, Zhu DL, Law CK. Morphology and burning rates of expanding spherical flames in H_2/O_2/inert mixtures up to 60 atmosphere. Proc Combust Inst 2000;28:1793–800.
[83] Brown MJ, McLean IC, Smith DB, Taylor SC. Markstein lengths of CO/H_2/Air flames using expanding spherical flames. Proc Combust Inst 1996;26:875–81.
[84] Prathap C, Ray A, Ravi MR. Investigation of nitrogen dilution effects on the laminar burning velocity and flame stability of syngas fuel at atmospheric condition. Combust Flame 2008;155:145–60.
[85] Sun H, Yang SI, Jomaas G, Law CK. High-pressure laminar flame speeds and kinetic modeling of carbon monoxide/hydrogen combustion. Proc Combust Inst 2007;31:439–46.
[86] Natarajan J, Lieuwen T, Seitzman J. Laminar flame speeds of H_2/CO mixtures: effect of CO_2 dilution, preheat temperature, and pressure. Combust Flame 2007;151:104–19.
[87] Hassan MI, Aung KT, Faeth GM. Properties of laminar premixed CO/H_2/air flames at various pressures. J Propul Power 1997;13:239–45.
[88] Vagelopoulos CM, Egolfopoulos FN. Laminar flame speeds and extinction strains rates of mixtures of carbon monoxide with hydrogen, methane, and air. Proc Combust Inst 1994;25:1317–23.
[89] McLean IC, Smith DB, Taylor SC. The use of carbon monoxide/hydrogen burning velocities to examine the rate of the CO+OH reaction. Proc Combust Inst 1994;25:749–57.
[90] Ratna Kishore V, Ravi MR, Ray A. Adiabatic burning velocity and cellular flame characteristics of H_2–CO–CO_2–air mixtures. Combust Flame 2011;158:2149–64.
[91] Yumlu VS. Prediction of burning velocities of carbon monoxide–hydrogen–air flames. Combust Flame 1967;11:190–4.
[92] Tien JH, Matalon M. On the burning velocity of stretched flames. Combust Flame 1991;84:238–48.